CHAPTER V
DIELECTRIC PROPERTIES OF POLYBENZOXAZINE-BARIUM STRONTIUM TITANATE COMPOSITES

5.1 Abstract

In this research, the composites with 0-3 connectivity of polybenzoxazine and barium strontium titanate ($Ba_{0.3}Sr_{0.7}TiO_3$) were fabricated by compression molding. The surface of BST particles was treated by using three different chemicals; 3-aminopropyl-trimethoxysilane, benzoxazine monomer and phthalocyanine. Then the effects of surface modification on the dispersion of BST particles and dielectric properties of the composites were studied. In addition, the dielectric properties as function of frequency, temperature and ceramic contents were also investigated. It was found that the dielectric constant of composites increased with increasing ceramic contents. By adding 80 wt% (48 vol%) of ceramic fillers, the dielectric constant was as high as 39. The dielectric constants of the composites were nearly stable with frequency range of 1 kHz–10 MHz and temperature range of 25-160°C. For the effects of surface modification, it was showed that the modified BST could disperse well in polybenzoxazine matrix. In the case of dielectric properties, the silane treating could improve dielectric constant of the composites compared with the others because it can form chemical bonds on the surface of BST powders. However, the composites with benzoxazine monomer and phthalocyanine treated BST powders showed the lower in dielectric loss because it could prevent the BST agglomeration in polybenzoxazine matrix more effectively than the silane coupling modification.

Keyword: Polybenzoxazine-barium strontium titanate composite, 0-3 connectivity, Dielectric properties, Surface modification, 3-aminopropyl-trimethoxysilane, Benzoxazine monomer, Phthalocyanine.

5.2 Introduction

Nowadays, there is an increasing demand for the use of embedded capacitors working at multi frequencies, particularly at high frequencies. The required properties of these materials are that they possess frequency-independent permittivities, low dielectric loss, good processability, and low cost [1]. Polymers are flexible, easy to process with low processing temperature, and possess a high dielectric breakdown field but generally suffer from low dielectric constant. On the other hand, ceramics possess a very high dielectric constant, but they are brittle, require high temperature processing, and have low dielectric strength. The integration of these two materials results in a new material with high dielectric constant, high breakdown field, and ease of processing to achieve high volume efficiency and energy storage density for applications of capacitors [2].

There are many different connectivity patterns have been designed in polymer-ceramic composites but the simplest type is the 0-3 connectivity pattern, which consists of a three-dimensionally connected polymer matrix filled with ceramic particles. The major advantages of the 0-3 type are its versatility in a variety of forms, including thin sheets and certain molded shapes. This type of composite is also easy to fabricate and is amenable to mass production [3]. In order to produce the 0-3 composites for high frequency applications, the composites must exhibit high permittivity with low dielectric loss. There are many research works that studied the dielectric behavior of 0-3 composites with different types of polymer matrices and ceramic fillers. Thermosetting polymers such as epoxy, phenolic resin, polyimide and polybenzoxazine, are generally used in the electronic application due to their high thermal stability and low viscosity properties. For ceramic filler, BST is one type of ferroelectric ceramic that is widely used due to its high dielectric constant and low loss properties at room temperature.

BST is a ferroelectric ceramic which is a related compound of barium titanate ($BaTiO_3$), formed by the substitution of strontium for barium, enabling BST to have a large dielectric constant, low dielectric loss at room temperature and high frequencies, compared with $BaTiO_3$ [4]. Thus BST has been considered to be an important material for high frequency applications. For the preparation of BST

powders, the sol-gel method is widely used because it provides powders with high chemical purity and homogeneity through a lower temperature process, grain size and shape control, and the avoidance of contamination of the materials. It also yields better stoichiometric control and nanopowder with high sinterability [5].

The problem that usually occurs in the composite with 0-3 connectivity is the agglomeration of ceramic particles which due to the incompatibility of polymers and ceramics. The surface of ceramics with residue hydroxyl groups, are hydrophilic in nature, while the polymers are hydrophobic. However, this problem can be avoided by treating the surface of ceramic before mixing in the polymer matrix. The surface modification method that widely used is silane coupling modification because of the variety of its functional groups. It has been reported that the uniform distribution of ceramic filler is the one of the factors that influences on the dielectric properties of the composite besides the dielectric properties of polymer matrix, the loading volume of ceramic and porosity in the composite [6].

However, the dielectric properties of the polymer-ceramic composite can be predicted by using various theoretical models such as Yamada model [7], Bruggeman formulae [8], Lichtenecker model [8], and Kerner expression modified by Jayasundere-Smith [9].

5.3 Experimental

5.3.1 Preparation of Barium Strontium Titante by Sol-Gel Process

Barium strontium titante ($Ba_{0.3}Sr_{0.7}TiO_3$) was prepared by dissolving 0.3 mole of barium acetate and 0.7 mole of strontium acetate separately in acetic acid, followed by the addition of methanol to each one. The solutions were mixed and stirred to obtain a clear solution. Then an equimolar amount of titanium (iv) n-butoxide was added into this mixture under vigorous stirring. When the solution became a gel, it was calcined by using 2-step thermal decomposition to decompose the solvent and crystallize $Ba_{0.3}Sr_{0.7}TiO_3$ powders.

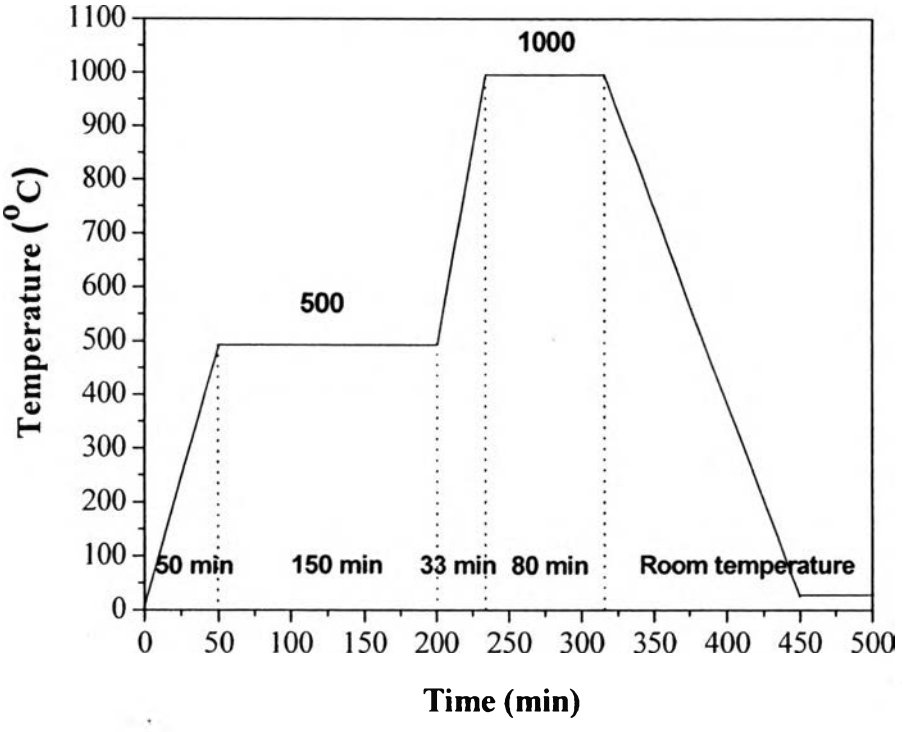

Figure 5.1 Temperature program for the 2-step thermal decomposition.

5.3.2 Surface Modification of BST Powder

5.3.2.1 Surface Modification by Silane Coupling

3-aminopropyl-trimethoxysilane (1g) was dissolved in water/ethanol (5ml/95ml) and the solution was then mixed with BST powders (40 g). This suspension was ultrasonicated at room temperature for 10 min and stirred at 70°C for 1 hr. The treated suspension was centrifuged and subsequently washed by ethanol and dried in a vacuum oven at 50°C. Finally, the coupling agent modified BST particles were obtained.

5.3.2.2 Surface Modification by Benzoxazine Monomer

In this method 5 wt% of aniline based benzoxazine monomer (BA-a monomer) was dissolved in THF. The solution was slowly added dropwise to stirring BST particle/THF slurry. Then the mixture was stirred for 1 hr and evaporated THF out at about 70°C. Lastly, treated BST was dried in a vacuum oven overnight in order to remove the residual solvent.

5.3.2.3 Surface Modification by Phthalocyanine

0.1 wt% of phthalocyanine powder was dissolved in DMAc solvent then added the solution into stirring BST particle/DMAc slurry. The mixture was then stirred for 1 hr and evaporated DMAc out at 200°C. After that the residual solvent was removed again by drying in a vacuum oven overnight.

5.3.3 Composite Preparation

In this part, the composite of aniline based polybenzoxazine and BST ceramic ($Ba_{0.3}Sr_{0.7}TiO_3$) was fabricated. Due to the much difference between the density of aniline based benzoxzine monomer and BST powder, the monomer and BST powder with 30, 50 and 80 wt% were firstly mixed together by melt mixing method to prevent the separation between two phases after fabrication step. Then the mixtures were fabricated as the composite specimens with the thickness of 1.5 mm and 15 mm in diameter by compression molding with the curing conditions given in Table 5.1.

Table 5.1 Temperature program for compression molding process

Temperature (°C)	Time (min)	Applied load (0.25 ton)
120	15	-
140	15	-
160	15	-
180	30	+
200	30	+
230	60	+

5.3.4 Characterizations

A crystal phase and structure of BST powder was analyzed by X-ray diffraction (Rigaku, model Dmax 2002) with Ni-filtered CuKα radiation operated at 40 kV and 30 mA with scan speed 5.00 deg/min from the 2θ range of 5.00 to 90.00 degree. Transmission electron microscope (TEM; H-7650, Hitachi) was used to observe particle size of sol-gel BST powder. Fourier transformation infrared spectrophotometer (NEXUS 670 FTIR) was used in order to measure functional groups and confirm the successful of the surface modification of BST ceramic.All spectra were recorded with absorbance mode in the wave number range of 4000-400 cm^{-1} and 32 scans per resolution. The apparent density of BST powder, benzoxzine monomer and polybenzoxazine were measured by pycnometer (Quantachrome, Ultrapycnometer 1000) under helium purge at pressure of 20 psi.

Thermal stability and degradation temperature of polybenzoxazine-BST composites were determined by a high resolution TG-DTA Pyris Diamond (Perkin Elmer). The mass change of samples was operated from 30°C to 800°C with a heating rate of 10°C/min under N_2 atmosphere. The distribution of BST powders in composites was observed by a scanning electron microscope (SEM; JSM-5200, Jeol) at voltage of 15 kV.

Dielectric measurement of composites was preformed with Hewlett-Packard 4194A Impedance/Gain-Phase Analyzer in parallel capacitance (C_p) mode, with frequency from 1 kHz to 10 MHz at room temperature. Before measurement, the composite specimens were coated with gold sputtering as electrodes. The dielectric constant (ε) of the composites was calculated from the measured thickness and capacitance by using the following equation:

$$\varepsilon = \frac{Cd}{\varepsilon_0 A} \qquad (5.1)$$

where C is the capacitance (F), ε_0 is the free space dielectric constant value (8.85×10^{-12} F/m), A is the capacitor area (m^2), and d is the thickness of specimen (m).

5.4 Results and Discussion

5.4.1 Barium Strontium Titanate Characterization

Morphology (particle size, shape and agglomeration) of the BST nanopowders prepared by sol-gel process was observed by TEM photograph as shown in Figure 5.2. The nanopowders were spherical shape with average size around 40-60 nm in diameter. It can also be observed that the particle size and shape distribution were nearly uniform and mostly agglomerate.

To confirm crystal structure of the sol-gel BST powder, X-ray diffraction (XRD) was investigated. From the XRD patterns shown in Figure 5.3, there are reflection peaks at 2θ values of 22.6°, 32.1°, 39.6°, 46.1°, 51.96°, 57.38° and 67.35° corresponding to (100), (110), (111), (200), (210), (211) and (220) set of diffraction planes, respectively. These results indicate that the BST gel transformed into the perovskite structure after calcination process. As observed from the XRD patterns that no peak splitting of (200)/ (002) at 2θ = 46.1° referring that the crystal structure of the BST particle is cubic structure [10]. However there were reflection peaks of $Ba(Sr)CO_3$ and $(Ba,Sr)_2Ti_2O_5CO_3$ (represented by *) at 2θ = 24.6° and 28.8°, respectively, which are undesirable phase in this sol-gel BST powder [11].

FTIR was investigated in order to confirm functional groups of the BST powder. As shown in Figure 5.4, there are three absorption peaks, the first one at 560 cm^{-1} due to the Ti-O stretching vibration of a TiO_6 octahedron, the second one at 1430 cm^{-1} which can be attributed to C=O stretching of carbonate ion impurities (CO_3^{2-}) in the BST powder and the other at 3422 cm^{-1} which corresponds to the antisymetric and symmetric OH stretching vibration indicating that hydroxyl groups (Ba-OH, Sr-OH) are detected on the surface of BST particles [12].

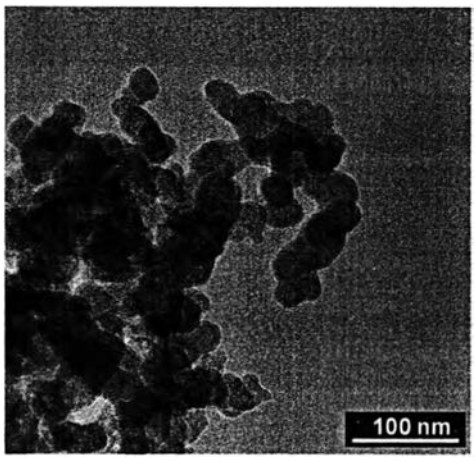

Figure 5.2 TEM micrographs of sol-gel BST powder.

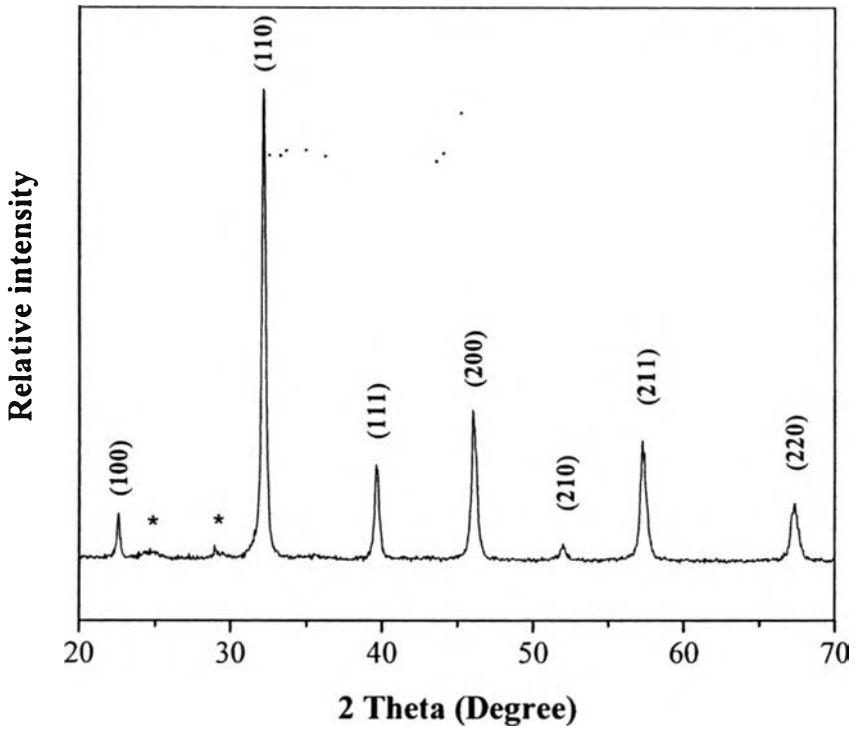

Figure 5.3 X-ray diffraction pattern of sol-gel BST powder.

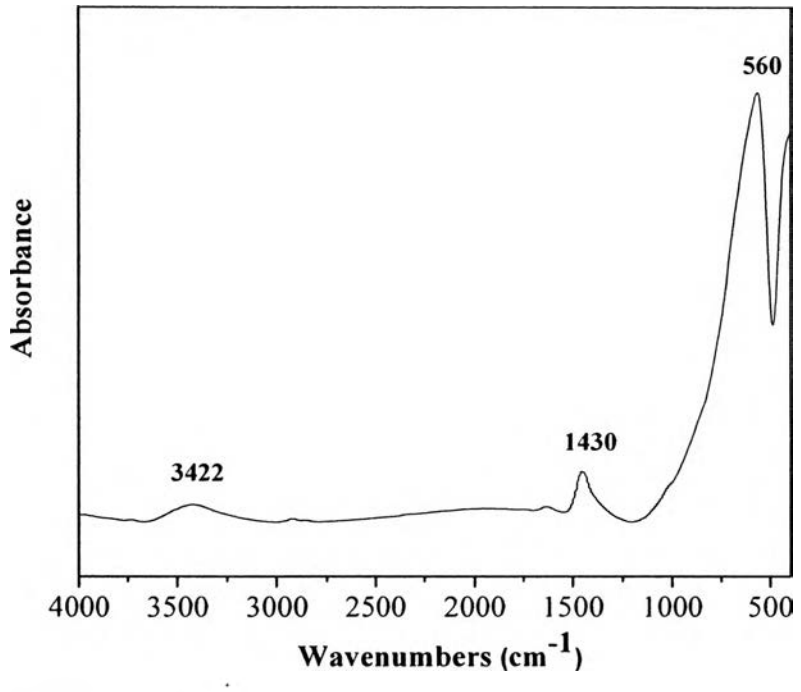

Figure 5.4 FTIR spectra of the BST powder.

5.4.2 Surface Modification of BST Powder

5.4.2.1 BST Powder Treated with Silane Coupling Agent

In order to improve the dispersion of BST ceramic in polybenzoxazine matrix to enhance the dielectric properties of the composite, the surface of BST particles was chemically modified with 3-aminopropyl trimethoxy silane by taking advantage of hydroxyl groups that detected on the surface of BST powders. Figure 5.5 shows the FTIR spectra of 3-aminopropyl trimethoxy silane treated BST powder and untreated BST powder. In comparison with the spectra of untreated BST powder, the spectra of 3-aminopropyl trimethoxy silane treated BST powder displayed new absorption band at 1110 cm^{-1} which is associated with the characteristic of Si-O-Si unit from the hydrolysis of silane. This result confirms that the silane coupling agent was hydrolyzed and reacted effectively onto the surface of BST particles [13].

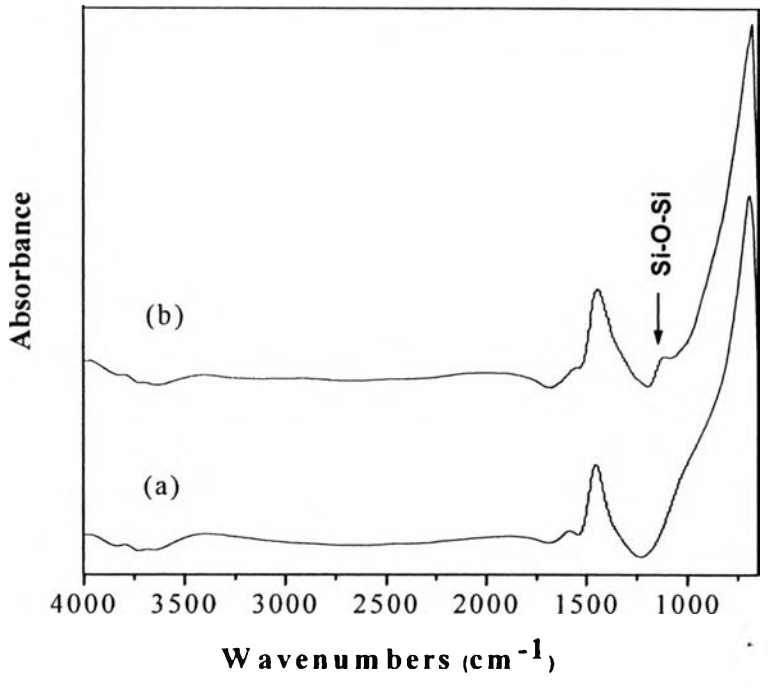

Figure 5.5 FTIR spectra: (a) BST powder and (b) 3-aminopropyl trimethoxy silane treated BST powder.

5.4.2.2 BST Powder Coated with Benzoxazine Monomer

To prevent the agglomeration of BST powders in polybenzoxazine matrix, surface coating of the ceramic powders by benzoxazine monomer is also investigated. From Figure 5.6, it can be observed that the spectrum of BST powder coated 5wt% BA-a monomer showed the absorption at wave number of 1230 cm^{-1} corresponding to asymmetric C-O-C stretching mode, the peaks at 1157 cm^{-1} and 1112 cm^{-1} which belong to C-N-C antisymmetric stretching mode of the BA-a monomer [14]. These results indicate that the monomer was already coated on the BST surface.

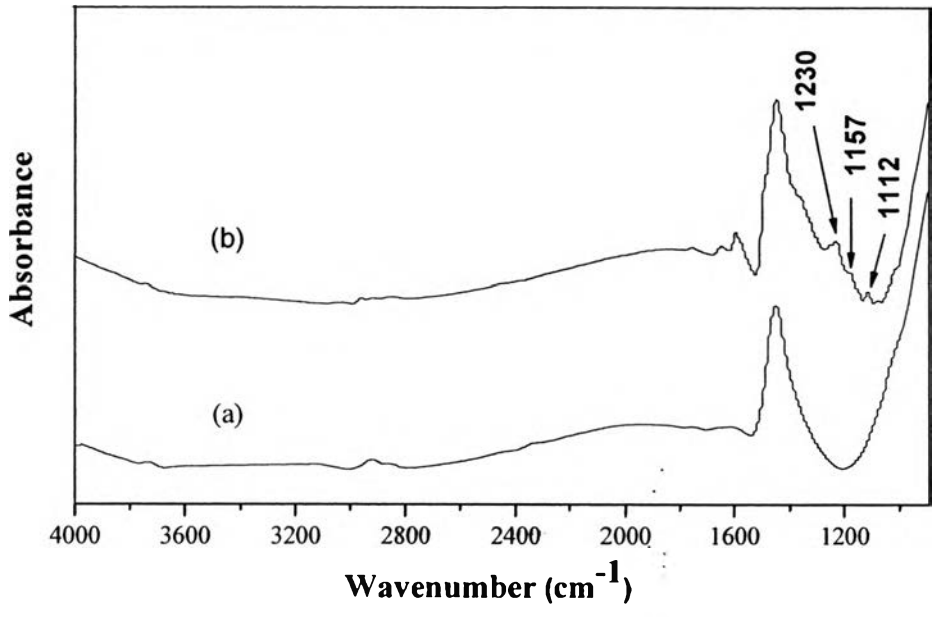

Figure 5.6 FTIR spectra of (a) BST powder (b) BST powder coated 5wt% BA-a monomer.

5.4.2.3 BST Powder Coated with Phtalocyanine

Figure 5.7 shows the FTIR spectra comparing between the phthalocyanine treated BST and untreated BST. There are the bands at the region of 1593 cm^{-1} and 1564 cm^{-1} which are the characteristic band of aromatic rings in the phthalocyanine structure [19]. However, there are no peaks that corresponding to the bond formation of C-Sr or C-Ba, imply that phthalocyanine did not form the bond on the surface of BST as expected but it just coated around the particles.

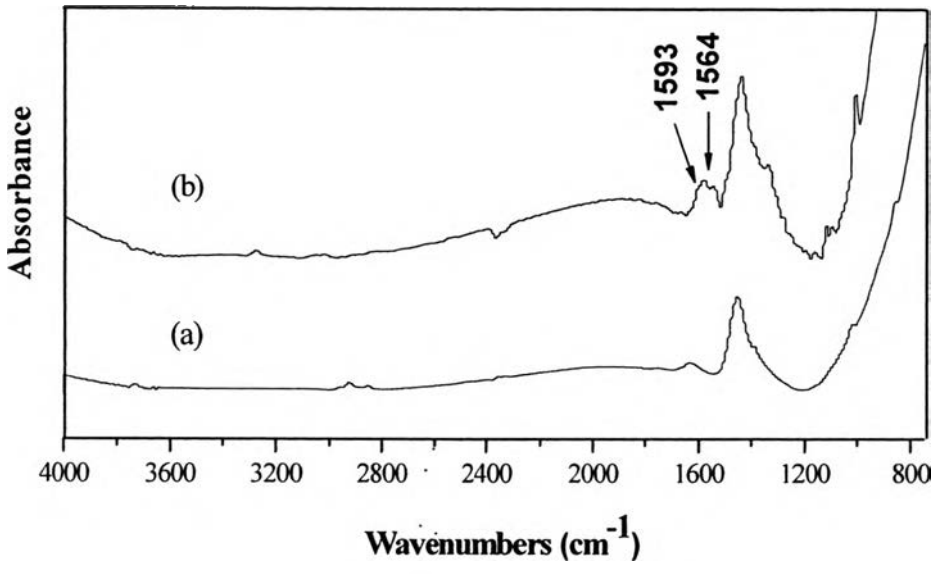

Figure 5.7 FTIR spectra of (a) BST powder (b) BST coated with phthalocyanine.

5.4.3 Polybenzoxazine- untreated BST Composite Characterization

5.4.3.1 Thermal Stability Measurement

TGA thermogram and thermal properties of the composites are shown in Figure 5.8 and Table 5.2. The degradation temperature and residual weight of composites were higher than pure polybenzoxazine and increased with the amount of BST contents. This is because the BST ceramic has high decomposition temperature compared with pure polybenzoxazine. Thus it can be concluded that the existence of BST powder can improve the thermal stability of the composites.

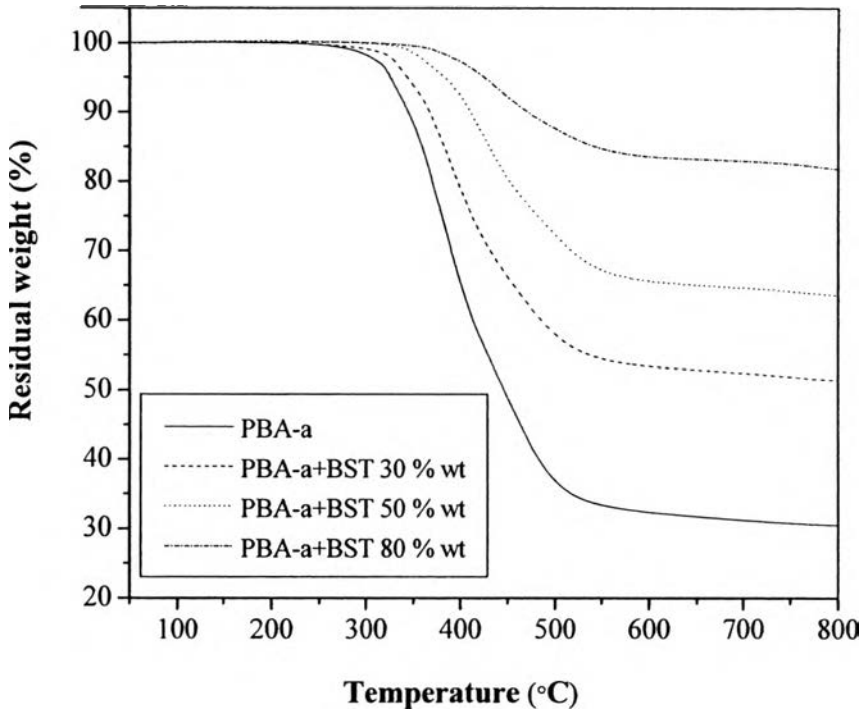

Figure 5.8 Thermo gravimetric analysis thermogram of polybenzoxazine-BST composites in nitrogen atmosphere.

Table 5.2 Thermal properties of polybenzoxazine-BST composites

Materials	T_{d5} (°C)	T_{d10} (°C)	Residual weight (%) at 800°C
Polybenzoxazine	325	344	30
Composite (BST 30wt%)	345	364	51
Composite (BST 50wt%)	382	408	63
Composite (BST 80wt%)	424	470	82

5.4.3.2 Density Measurement

The density of polybenzoxazine, calcined BST powder and the composites at various BST powder loading was measured by pyconometer. The theoretical density of material was calculated by using equation (5.2):

$$\rho_T = (1-\phi)\rho_p + V\rho_c \qquad (5.2)$$

where ρ_c is the filler density, ρ_p is the polymer matrix density and ϕ is the volume fraction of filler. Density of polybenzoxazine and calcined BST powder is 1.23 and 5.17 g/cm^3, respectively. The measured densities of the composites with increasing ceramic volume fraction are summarized in Table 5.3. And Figure 5.9 shows the variation of the theoretical density and measured density of the composites. It was found that the measured density of 30 wt% BST composite can fit well with the theoretical density while the density of composite with 50 wt% and 80 wt% BST are lower than the calculated. This difference between the calculated or theoretical values and the measured values is presumably due to defects or voids occurring during fabrication process.

Table 5.3 Densities of the composites at various BST contents

Composites	Volume fraction	Density (g/cm^3)
30 wt% BST	0.093	1.597
50 wt% BST	0.192	1.933
80 wt% BST	0.488	2.867

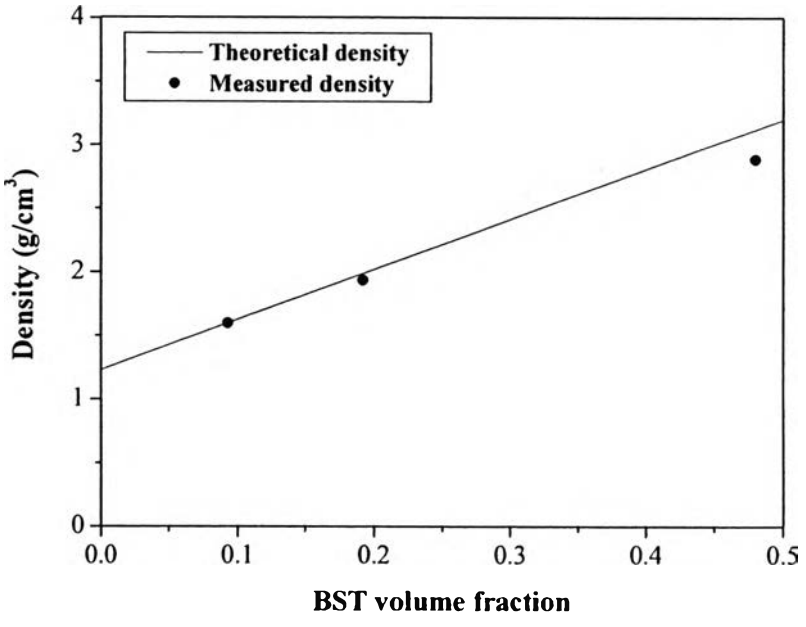

Figure 5.9 Comparison between measured density (●) and theoretical density (—) as a function of BST volume fraction.

5.4.3.3 Barium Strontium Titanate Distribution

The distribution of BST powders in the polybenzoxazine matrix was investigated by SEM micrographs. Figure 5.10 (a)-(c) shows the cross-section of the composites with different BST loadings. The white and gray colors represent the filler and the polybenzoxazine matrix, respectively. From the micrographs, it reveals that the BST powder distribution was not uniform even in the lowest content of BST fillers (30 wt %) and the agglomeration and pores (represent by black color) tended to form when the filler loading volume increased. The agglomeration of BST is formed by the high surface energy of the sol-gel BST nanoparticles.

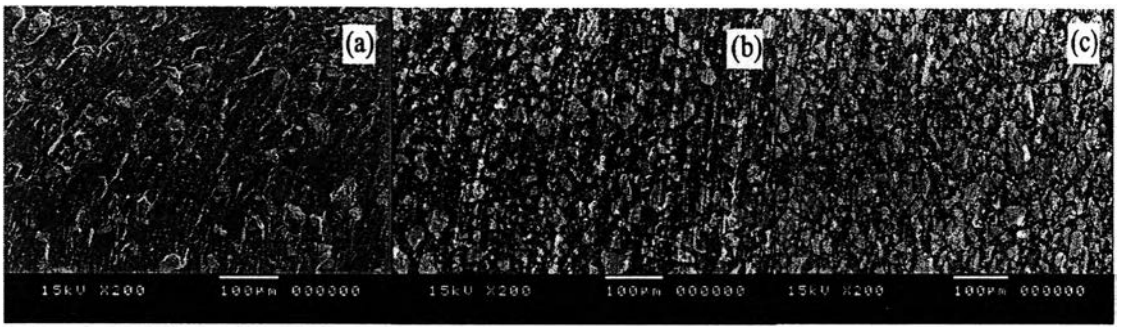

Figure 5.10 SEM micrographs of the composites with (a) 30 wt%, (b) 50 wt%, and (c) 80 wt%.

5.4.3.4 Dielectric Properties of Composites

The dielectric constant and dielectric loss of the composites with 30 wt%, 50 wt%, and 80 wt% of BST as a function of frequency, from 1 kHz-10 MHz are shown in Figure 5.11 and 5.12, respectively. From Figure 5.11, it can be seen that at the same frequency, the composite dielectric constants increased with the volume fraction of the BST ceramic powders. At higher ceramic filler loading volume, the ceramics come closer then the dipole-dipole interaction increase and contribute to higher dielectric constant [15]. In this work the composite with 80 wt% of BST showed the dielectric constant as high as 39 at 1 kHz, about eight times of 4.9 for polybenzoxzazine. However, it was found that the loss tangents of all composites are greater than pure polybenzoxazine and tend to increase at higher ceramic content. The increasing of the loss tangent value was attributed to the formation of porosity in the specimens.

For the temperature dependence as shown in Figure 5.13 and 5.14, dielectric constant and loss tangent of the composites showed the temperature independence up to the glass transition temperature of the polymer. At the themperature above T_g of polybenzoxzine, the dielectric constant and loss tangent slightly increased. The increase of dielectric constant and dielectric loss was attributed to the improvement of the dipole orientation polarization of the polymer chains at temperature above T_g. In addition, the segmental mobility of the polymer also facilitated polarization of ceramic filler resulting in the dielectric constant enhancement of the composites [16].

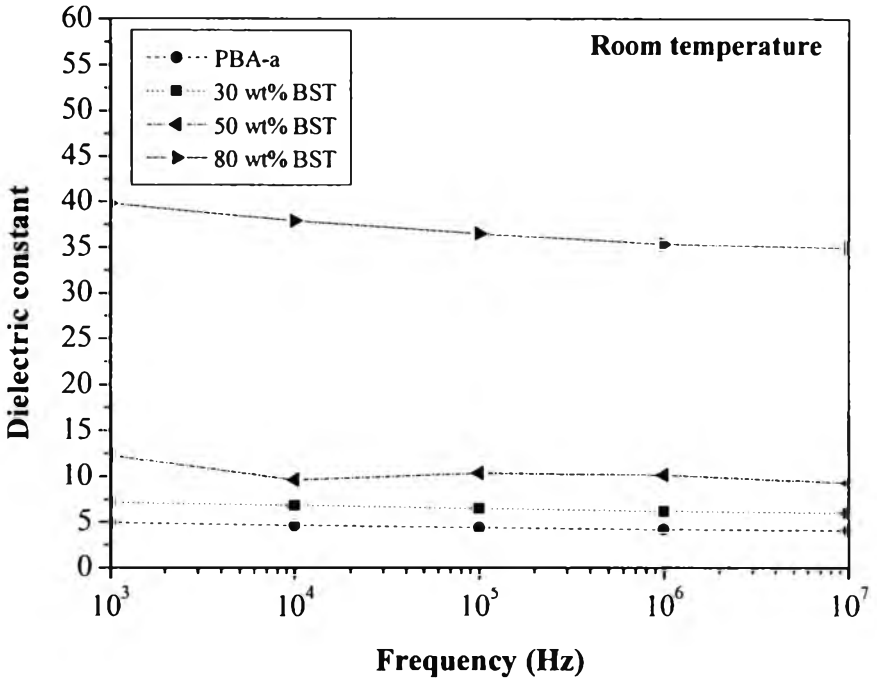

Figure 5.11 Frequency dependence of dielectric constant for the composites at various BST contents.

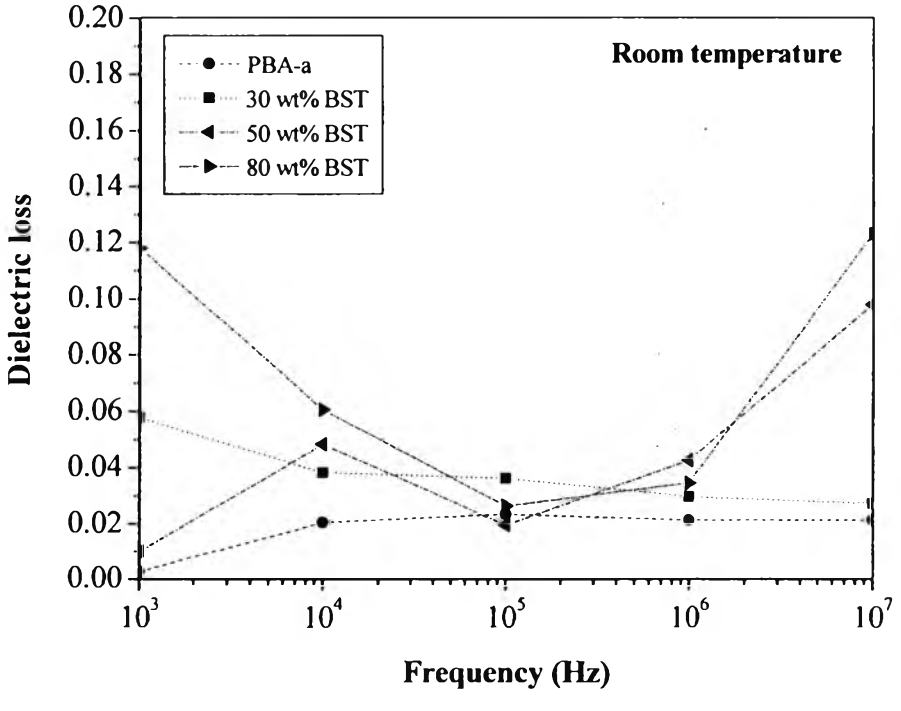

Figure 5.12 Frequency dependence of dielectric loss for the composites at various BST contents.

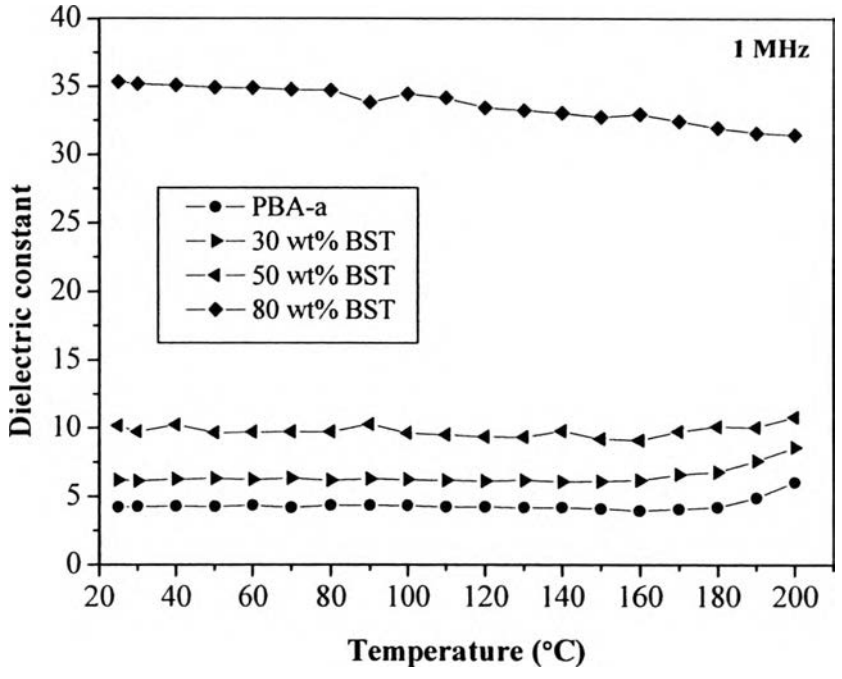

Figure 5.13 Temperature dependence of dielectric constant for the composites at various BST contents.

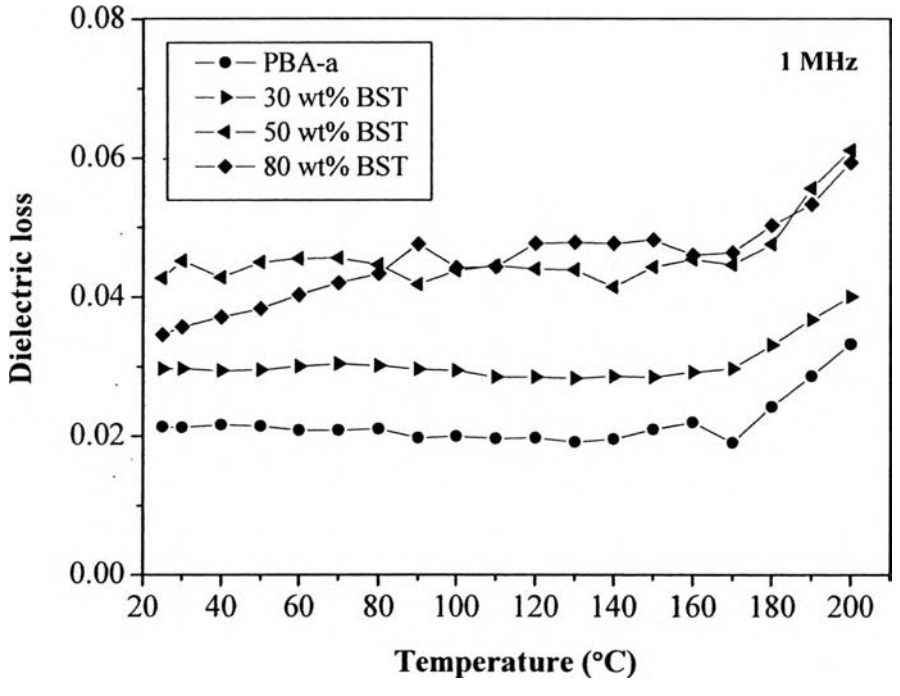

Figure 5.14 Temperature dependence of dielectric loss for the composites at various BST contents.

5.4.4 Experimeantal Data Fitting

There are many theoretical models have been proposed and used for predicting the dielectric constant of 0-3 connectivity composite comparing with experimental results. The models that widely used such as Yamada model, Lichtenecker model, Bruggeman model and Kerner expression modified by Jayasundere-Smith (J-S prediction), as shown in Figure 5.15. The equations of these models are described as follow:

Yamada model
$$\varepsilon = \varepsilon_p \left[\frac{\eta\phi(\varepsilon_c - \varepsilon_p)}{\eta\varepsilon_p + (\varepsilon_c - \varepsilon_p)(1+\phi)} \right] \quad (5.3)$$

Lichtenecker model
$$\log\varepsilon = \log\varepsilon_p + \phi\log\left(\frac{\varepsilon_c}{\varepsilon_p}\right) \quad (5.4)$$

Bruggeman formulae
$$\frac{\varepsilon_c - \varepsilon}{\varepsilon_c - \varepsilon_p}\left(\frac{\varepsilon_p}{\varepsilon}\right)^{1/3} = 1-\phi \quad (5.5)$$

Kerner expression
$$\varepsilon = \frac{\varepsilon_p\phi_p + \varepsilon_c\phi_c[3\varepsilon_p/(\varepsilon_c + 2\varepsilon_p)][1 + 3\phi_c(\varepsilon_c - \varepsilon_p)/(\varepsilon_c + 2\varepsilon_p)]}{\phi_p + \phi_p(3\varepsilon_c)/(\varepsilon_p + 2\varepsilon_c)[1 + 3\phi_c(\varepsilon_c - \varepsilon_p)/(\varepsilon_c + 2\varepsilon_p)]} \quad (5.6)$$

where ε is the dielectric constant of the composites, ε_p and ε_c refer to the dielectric constants of the polymer matrix and the BST ceramic, respectively, ϕ is the volume fraction of ceramic and η is a shape parameter [7], [8], [9]. For the calculation, the dielectric constant of $Ba_{0.3}Sr_{0.7}TiO_3$ (ε_c = 308) [17] and the pure polybenzoxazine (ε_p = 4.94) were used. The dielectric constants were measured at room temperature (~25°C) and 1 kHz.

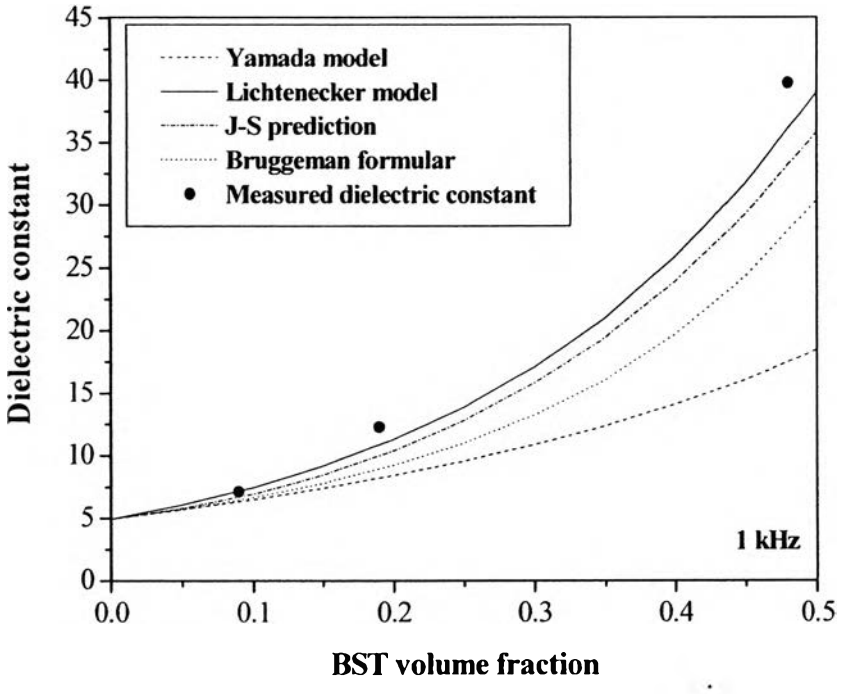

Figure 5.15 Plot of theoretical models and the measured dielectric constant for different BST volume fractions at room temperature and 1 kHz.

From the comparison between the experimental data and four theoretical models, as shown in Figure 5.15, it was found that the measured dielectric constants of the PBA-a-BST composites are higher than those calculated from Yamada, Bruggeman and J-S prediction. It is, however, noted that the measured dielectric constants show a tendency to fit well with the Lichtenecker model. Lichtnecker model is more commonly known as the Log Law, it considers the composite as a random mixture of nearly spherical inclusions. However the Lichtenecker's equation does not consider the fitting factor which depends on the material used in the system [18].

5.4.5 Polybenzoxazine-modified BST Composite Characterization

5.4.5.1 Effect of Surface Modification on BST powder Distribution

SEM micrographs were investigated to study the effect of BST surface modification on the ceramic dispersion in polybenzoxazine matrix with various BST volume fractions. Figure 5.17-5.19 (a)-(d) show microstructure of the composites containing 30wt%, 50 wt% and 80 wt% of BST fillers that were untreated, treated with silane coupling agent, treated with BA-a monomer and treated with phthalocyanine, respectively. The SEM micrographs reveal that the dispersion of the modified BST powders was improved in every fraction of BST powders, especially at 30 wt% BST composite.

In comparison between silane coupling agent, BA-a monomer and phthalocyanine modification of BST, it was observed that the composites with phthalocyanine and benzoxazine monomer modification showed the best in the ceramic dispersion improvement compared with the silane coupling method. Because the molecules of phthalocyanine and benzoxazine monomer are composed of the aromatic rings which are bulky group, as shown in Figure 5.16, due to this way they could prevent the BST particles to come closer. The silane coupling agent could not work effectively as expected because it might react with each other instead of BST surface in modification step.

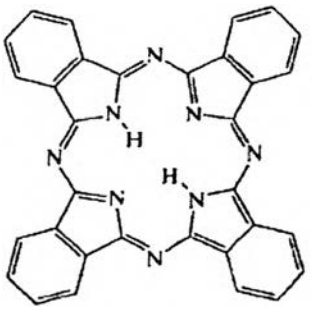

Phthalocyanine

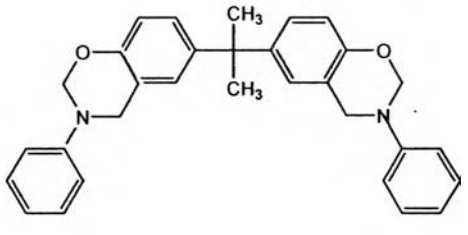

Benzoxazine monomer

Figure 5.16 Structure of metal-free phthalocyanine and benzoxazine monomer.

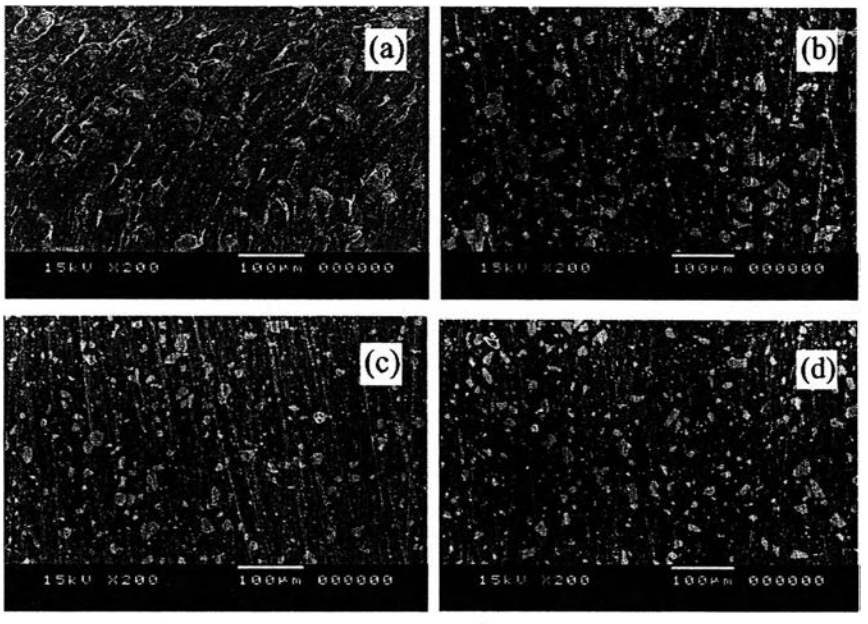

Figure 5.17 SEM micrographs of polybenzoxazine-BST composites at 30%wt of BST with (a) untreated BST powders, (b) silane treated BST powders, (c) BA-a monomer treated BST powders and (d) phthalocyanine treated BST powders .

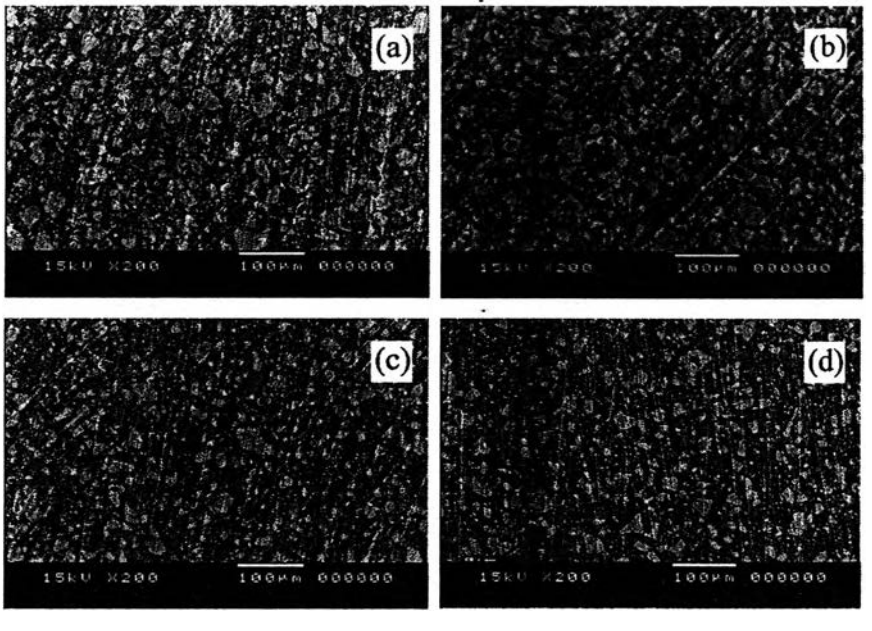

Figure 5.18 SEM micrographs of polybenzoxazine-BST composites at 50%wt of BST with (a) untreated BST powders, (b) silane treated BST powders, (c) BA-a monomer treated BST powders and (d) phthalocyanine treated BST powders .

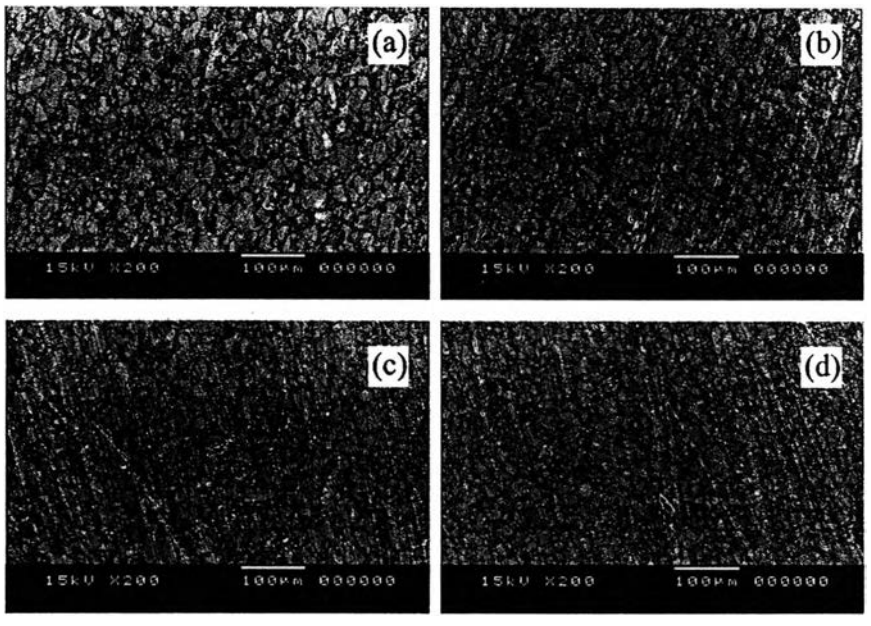

Figure 5.19 SEM micrographs of polybenzoxazine-BST composites at 80%wt of BST with (a) untreated BST powders, (b) silane treated BST powders, (c) BA-a monomer treated BST powders and (d) phthalocyanine treated BST powders .

5.4.5.2 Effect of Surface Modification on Dielectric Properties of Composites

Figure 5.20 to 5.25 illustrate the comparisons of dielectric constant and dielectric loss of the composites with different BST surface modification method at various BST contents. Considering the dielectric constants of the composites at 30wt%, 50wt% and 80 wt% in Figure 5.20, 5.20 and 5.22, respectively, it was found that the silane coupling modification can improve in the dielectric constant of composites. While the phthalocyanine and the benzoxazine monomer modification did not show significant in dielectric constant improvement. Because silane coupling agent can form chemical bonds on the surface of BST powders due to this way the polarizability in the system could be enhanced, resulting in the increasing of the dielectric constant. In the case of dielectric losses of the composites at 30wt%, 50wt% and 80 wt%, shown in Figure 5.23, 5.23 and 5.25, respectively, it can be seen that all three methods of surface modification could obviously lower the dielectric loss of the composites compared with the untreated BST composites. In comparison among the three surface modification methods, it was found that the phthalocyanine and benzoxazine monomer could lower the loss tangent of the composites than the silane coupling method, especially at 30 wt% of BST. The lower in dielectric loss was due to the BST dispersion enhancement of the phthalocyanine and benzoxazine monomer, consequent in the lower of porosity in the composites. Because it was reported that porosity is the important factor that mainly increases the loss in the composite system. The porosity could be generated from the segregation of different surfaces between polymer matrix and ceramic particles and will be large when composite was pressed by mechanical loading.

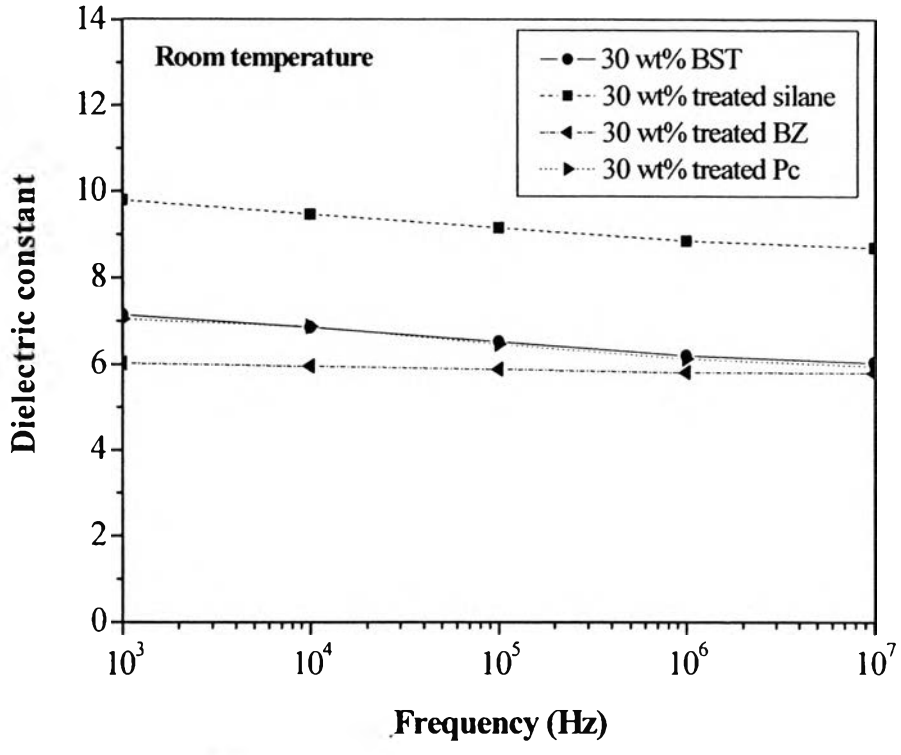

Figure 5.20 Frequency dependence of dielectric constant for the 30%wt BST composites with different BST surface modification methods.

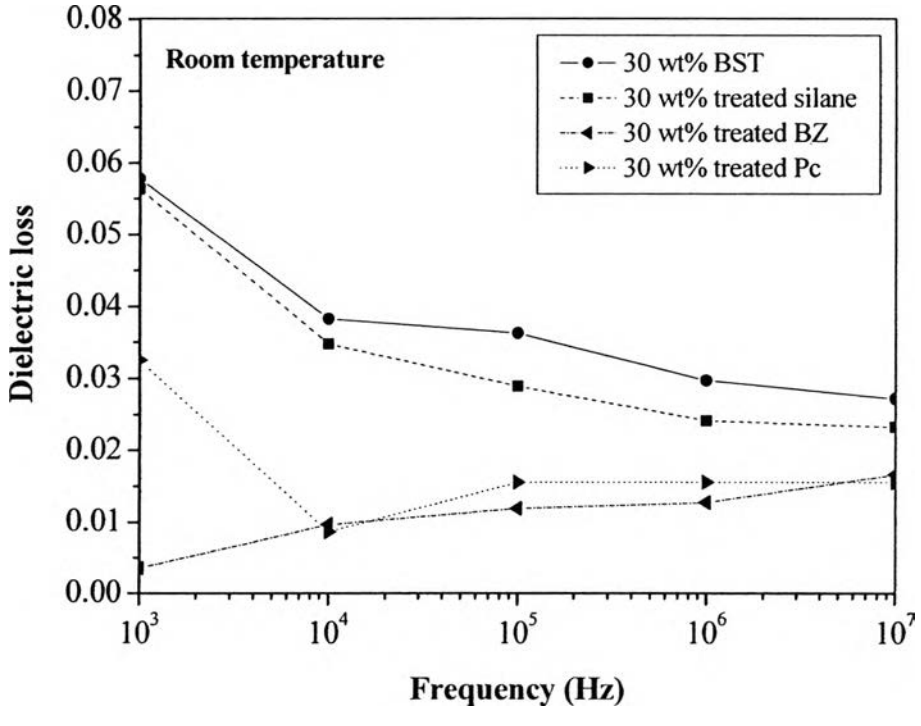

Figure 5.21 Frequency dependence of dielectric loss for the 30%wt BST composites with different BST surface modification methods .

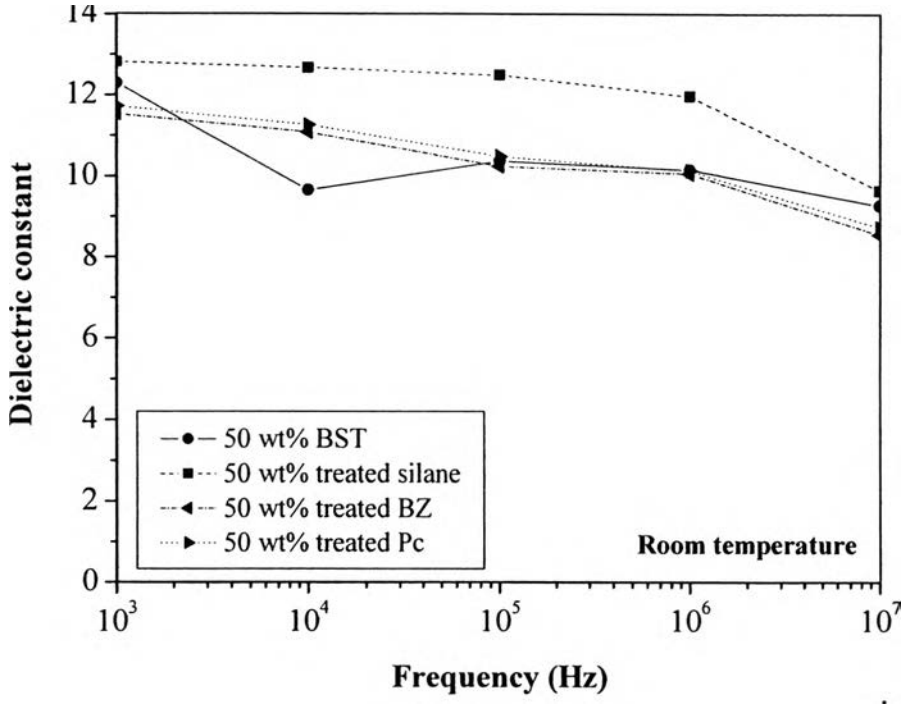

Figure 5.22 Frequency dependence of dielectric constant for the 50%wt BST composites with different BST surface modification methods .

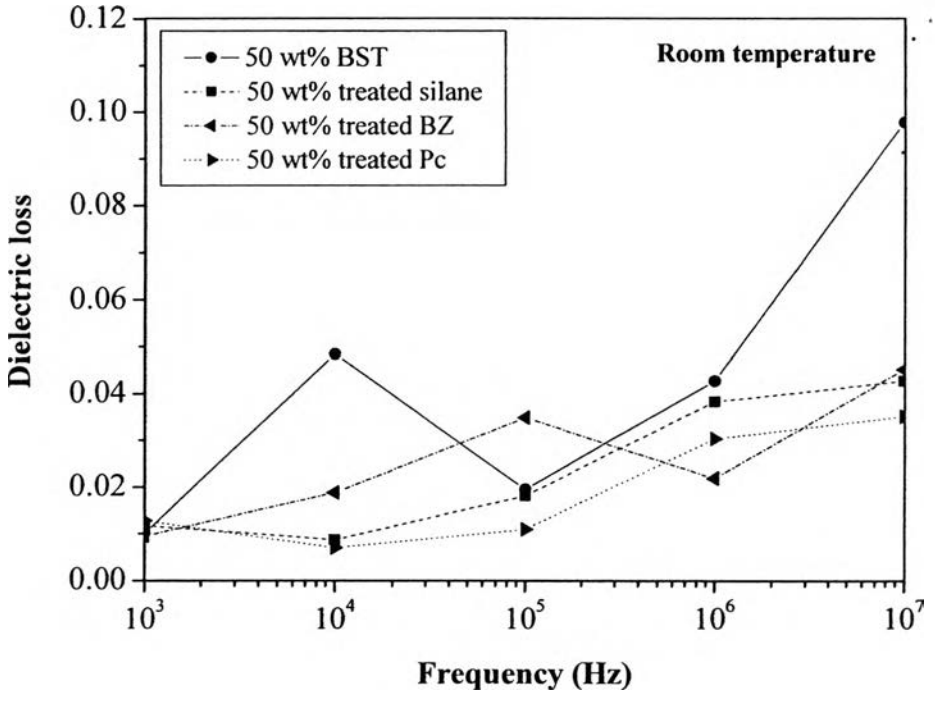

Figure 5.23 Frequency dependence of dielectric loss for the 50%wt BST composites with different BST surface modification methods .

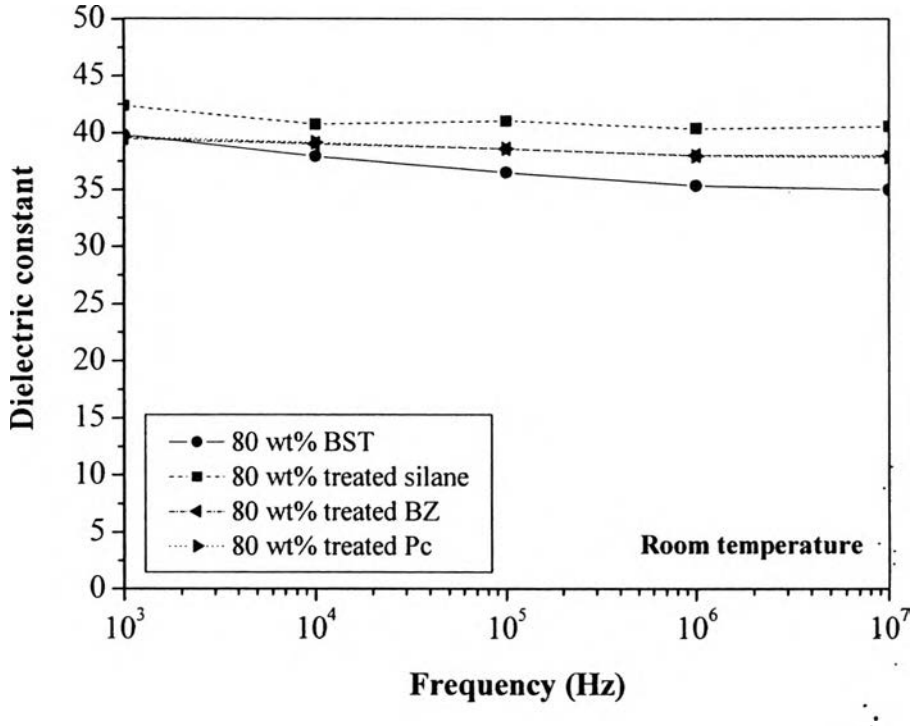

Figure 5.24 Frequency dependence of dielectric constant for the 80%wt BST composites with different BST surface modification methods .

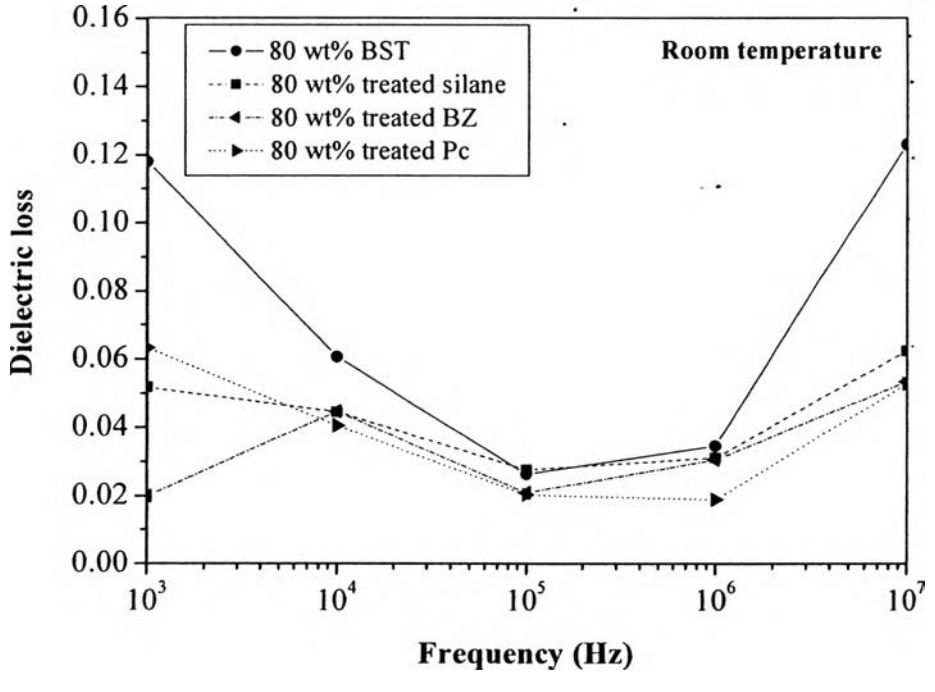

Figure 5.25 Frequency dependence of dielectric loss for the 80%wt BST composites with different BST surface modification methods .

5.5 Conclusions

The dielectric properties of the composites were influenced by many factors such as ceramic volume fraction and the distribution of ceramic powders. In this work, the composite with 80 wt% or 48 vol% of BST showed the dielectric constant as high as 39 which about eight times of 4.9 for pure polybenzoxazine at 1kHz. The dielectric constants of the composites were nearly stable with frequency range of 1 kHz–10 MHz. The positive temperature coefficient (PTC) of dielectric constant was nearly zero in the temperature range of 25-160°C, which indicated the low relaxation behavior. It was found that the composites in this work could fit well with the Lichtnecker model which considers the composite as a random mixture of nearly spherical inclusions. For the effects of surface modification on BST powders, it was observed that the modified BST surface could disperse well in polybenzoxazine matrix compared with the unmodified BST powders. And considering in dielectric properties, it was found that silane modification could improve dielectric constant of the composites compared with others. However, the composites with benzoxazine monomer and phthalocyanine treated BST powders showed the lower in dielectric loss because it could prevent the BST agglomeration in the polymer matrix more effectively than the silane coupling modification.

5.6 Acknowledgements

The authors thank the partial scholarship and partial funding of the research work provided by the Petroleum and Petrochemical College; the National Excellence Center for Petroleum, Petrochemical, and Advanced Materials, Thailand and research grant from the Government Research Budget Year 2005-2007 (GRB_๔๗_๕๐_๖๓_๐๔). The authors also gratefully acknowledge Dr. Pitak Laoratanakul and MTEC staffs for useful assistance and instrument for characterizations.

5.7 References

[1] Pant, H.C., Patra, M.K., Verma, A.,Vadera, S.R., and Kumar, N. (2006). Study of the dielectric properties of barium titanate-polymer composites. Acta Materialia, 54, 3163-3169.

[2] Bai , Y., Cheng, Z.Y., Bharti, V., Xu, H.S., and Zhang, Q.M. (2000). High-dielectric constant ceramic powder polymer composites. Applied Physics Letters, 76(25), 3804-3806.

[3] Lee, H.G., and Kim, H.G. (1989). Ceramic particle size dependence of dielectric and piezoeletric properties of piezoelectric ceramic-polymer composites. Journal of Applied Physics, 67(4), 2024-2028.

[4] Lu, O., Chen, D., and Jiao, X. (2003). Preparation and characterization of $Ba_{1-x}Sr_xTiO_3$ (x=0.1, 0.2) fibers by sol-gel process using catechol-complex titanium isopropoxide. Journal of Alloys and Compounds, 358, 76-81.

[5] Yang, W., Chang, A., and Yang, B. (2002). Preparation of barium strontium titanate ceramic by sol-gel method and microwave sintering. Journal of Materials Synthesis and Processing, 10(6), 303-309.

[6] Li Li, Takahashi, A., Hao, J., Kikuchi, R., Hayakawa, T., Tsurumi, T.A., and Kakimoto, M.A. (2005). Novel polymer-ceramic nanocomposite based on new concepts for embedded capacitor application (I). IEEE transactions on components and packaging technologies, 28, 754-759.

[7] Yamada, T., Ueda, T., and Kitayam, T. (1982). Piezoelectricity of a high–content lead zirconate titanate/polymer composite. Journal of Applied Physics, 53(6), 4328-4332.

[8] Frost, N.E., McGrath, P.B., and Burns, C.W. (1996). Effect of fillers on the dielectric properties of polymers. IEEE International Symposium on Electrical Insulation, 300-303.

[9] Jayasundere, N., and Smith, B.V. (1993). Dielectric constant for binary piezoelectric 0-3 composites. Journal of Applied physics, 73 (5), 2462-2466.

[10] Viswanath, R.N., and Ramasamy, S. (1997). Preparation and ferroelectric phase transition studies of nanocrystalline $BaTiO_3$. Nano Stuctured Materials, 8(2), 155-162, 1997.

[11] Mao, C., Dong, X., and Zeng, T. (2007). Synthesis and characterization of nano-crystalline barium strontium titanate. Materials Letters, 61, 1633-1636.

[12] Hwang, U.Y., Park, H.S., and Koo, K.K. (2004). Low-temperature synthesis of fully crystallized spherical $BaTiO_3$ particles by the gel-sol method. Journal of the American Ceramic Society, 87(12), 2168-2174.

[13] Xie, S.H., Zhu, B.K., Wei, X.Z., Xu, Z.K., and Xu, Y.Y. (2005) Polyimide/$BaTiO_3$ composites with controllable dielectric properties. Composites: Part A, 36, 1152–1157.

[14] Ishida, H.and Rodriguez, Y. (1995). Curing kinetics of a new benzoxazine-based phenolic resin by differential scanning calorimetry. Polymer, 36(16), 3151-3158.

[15] Kuo, D.H., Chang, C.C., Su, T.Y., Wang, W.W., and Lin, B.Y. (2001). Dielectric behaviours of multi-doped $BaTiO_3$/epoxy composites. Journal of the European Ceramic Society, 21, 1171-1177.

[16] Xie, S.H., Zhu, B.K., Wei, X.Z., Xu, Z.K., and Xu, Y.Y. (2004). Polyimide/$BaTiO_3$ composite with controllable dielectric properties. Composite: Part A, 36, 1152-1157.

[17] Panomsuwan, G., Manuspiya, H., and Ishida, H. (2006). Electrical properties of barium strontium titanate/polybenzoxazine composite with 0-3 connectivity. M.S.Thesis, The Petroleum and Petrochemical College, Chulalongkorn University, Bangkok, Thailand

[18] Rao, Y., Qu, J., and Marinis, T. (2000). A precise numerical prediction of effective dielectric constant for polymer–ceramic composite based on effective-medium theory. IEEE Transactions on components and packaging technologies, 23(4), 680-683.

[19] Kantar, C., Akdemir, N., A˘gar, E., Ocak, N., Sasmaz, S. (2008). Microwave-assisted synthesis and characterization of differently substituted phthalocyanines containing 3,5-dimethoxyphenol and octanethiol moieties. Dyes and Pigments, 76, 7-12.